Appl. Phys. B 80, 193–198 (2005)
DOI: 10.1007/s00340-004-1702-4

Applied Physics B
Lasers and Optics

T.-J. WANG✉
J.-S. CHUNG

Wavelength-tunable polarization converter utilizing the strain induced by proton exchange in lithium niobate

Institute of Electro-Optical Engineering, National Taipei University of Technology,
No. 1, Sec. 3, Chung-Hsiao E. Rd., Taipei 10651, Taiwan, P.R. China

Received: 15 June 2004/Final version: 13 October 2004
Published online: 8 December 2004 •

ABSTRACT A new wavelength-tunable polarization converter utilizing the strain induced by proton exchange is demonstrated in x-cut $LiNbO_3$. The light polarization is converted by the strain-optic effect through the phase-matched coupling of two orthogonal polarizations. The stress-applying structure is designed to be composed of several proton-exchanged strip regions for maximization of the stress distribution. The principle of birefringent chain filters is utilized to design the device structure in order to avoid the requirement of large stress, which results in serious cracks on the substrate surface. The overlap integral between the optical field distribution and the stress distribution can be enhanced simply by prolonging the proton-exchange time. Besides, the stress distribution and its strength in the stress-applying structure can be fine tuned without affecting the waveguide characteristics such that the principle of the birefringent chain filters is completely satisfied. Therefore, the polarization-conversion efficiency can be optimized when utilizing this exclusive stress-tuning ability. By the thermal-optic effect, the wavelength of maximum conversion can be tuned at a rate of $-0.115\,\mathrm{nm/°C}$ with a maximum conversion efficiency of 92.41%. The proposed polarization converter has the advantages of adequate stress distribution and strength, high parameter-tuning feasibility, low propagation loss, easy fabrication, and low fabrication cost.

PACS 42.82.-m

1 Introduction

In optical integrated circuits, polarization manipulation is an important issue to eliminate the polarization dependence of device performance and achieve coherent signal detection. The light polarization can be converted by the coupling of two orthogonal polarizations through a change of an optical property in the material or an asymmetry in the waveguide structure. For the former, the tilt of waveguide principal axes or the non-zero off-diagonal elements of the dielectric tensor can be induced by physical phenomena, such as electro-optic [1], acousto-optic [2], magneto-optic [3], or strain-optic effects [4–6]. As to the latter, various asymmetric waveguide structures, such as asymmetric-loaded waveguides [7] and angle-faced waveguides [8], are utilized to produce the coupling of weakly hybrid polarization modes. In order to have an efficient polarization conversion, the device parameters must be designed to achieve the phase-matched coupling and the maximal overlap integral between the input optical field and the distribution of the physical field or the interaction structure.

Previously, several polarization converters based on the strain-optic effect have been reported. Tang et al. [4] utilized the shear strain induced by the thermal mismatch between substrate and 1.5-μm-thick SiO_2 strips to produce an off-diagonal index change in lithium tantalate. The periodic shear strain is formed by electron-beam evaporation of a thick SiO_2 film at 300 °C and then reactive-ion etching the film as strips to relax partial compressional strain. The resultant strain distribution is concentrated near the surface and is not easy to extend its range in the depth direction. Because the optical field at longer wavelength has a larger mode size, a shallow strain distribution has a smaller overlap integral with this optical field and reduces the polarization-conversion efficiency at the longer wavelength. Lang et al. [5] reported a polarization converter on a glass substrate using integrated asymmetric ion-exchanged stress segments. Jung et al. [6] used the same principle as [4] to produce a wavelength-tunable polarization converter in lithium niobate.

An ideal stress-applying structure in the polarization converter based on the strain-optic effect must satisfy the following conditions:

- The strain-applying structure can produce a large strain.
- The induced strain distribution has an adequate and tunable depth to increase the overlap integral between the optical field distribution and the strain distribution.
- The index of the strain-applying structure must be smaller than that of the waveguide to avoid damaging the lateral optical confinement of the waveguide.

Previous works only partially satisfy these requirements. In this paper, a new integrated-optic wavelength-tunable polarization converter in x-cut lithium niobate, which completely satisfies these three requirements, is presented. Since lithium niobate has excellent electro-optic, acousto-optic, piezo-electric, and nonlinear-optic effects, various versatile functional devices have been successfully demonstrated on

✉ Fax: +886-2-8773-3216, E-mail: f10939@ntut.edu.tw

this material. Different fabrication techniques in lithium niobate are used to satisfy the requirement of exclusive characteristics in different device regions. The stress produced by proton exchange is utilized to induce the polarization conversion by the tilt of waveguide principal axes. The dependence of optical properties, such as the birefringence and the tilt of the waveguide principal axes, on the proton-exchange conditions is discussed. The polarization converter is designed such that, for both polarizations, the stress-applying structure has a lower index than that of the waveguide to avoid the lateral leakage of optical field toward the stress-applying structure. The effects of proton-exchange depth on the polarization-conversion efficiency and the thermal-optic tuning characteristics of the proposed polarization converter are demonstrated. In comparison with the previous works [4–6], the proposed polarization converter has many advantages, such as adequate stress distribution and strength, high parameter-tuning feasibility, low propagation loss, easy fabrication, and low fabrication cost.

2 Device design and fabrication

2.1 *Design*

The proposed polarization converter is shown schematically in Fig. 1. Because the stress caused by the proton-exchanged region is stronger near the region boundary, the stress-applying structure is designed to be composed of several proton-exchanged strip regions with length l, width W_s, and period Λ. The tilt of waveguide principal axes, as shown in Fig. 2, is induced by the stress through the strain-optic effect. The waveguide birefringence and the tilt angle of waveguide principal axes are dependent on the proton-exchange conditions and the geometrical parameters, such as length l, width W_s, and period Λ. The polarization conversion can be achieved through the coupling of two orthogonal polarization modes. In order to have a 90°-polarization rotation (TE → TM or TM → TE), the required tilt angle of waveguide principal axes is 45°, which can be achieved by a quite large stress. Such a large stress usually results in cracks on the substrate surface and is unfeasible in the device fabrication. This difficulty can be overcome by using several half-wave sections with an alternating tilt angle of waveguide principal axes ($\pm\alpha$) to successively rotate the polarization angle for a 90°-polarization rotation. For phase-matched coupling between the TE- and the TM-polarized modes, the length of the half-wave section L_S must be set as

$$L_S = \frac{\lambda}{2\,|n_{TE}(\lambda) - n_{TM}(\lambda)|}\,, \tag{1}$$

where λ is the free-space wavelength and n_{TE} and n_{TM} are the effective indices for the TE- and the TM-polarized modes. According to the principle of birefringent chain filters [9], the overall polarization-rotation angle (θ) at the end of the mth half-wave section can be expressed as

$$\theta = (-1)^m 2m\alpha\,. \tag{2}$$

For 90°-polarization rotation, section number m can be found when α is known. For example, when the section number is 3 (4), the corresponding α is 15° (11.25°). The proposed polarization converter is fabricated on an x-cut, z-propagating $LiNbO_3$ substrate. In this device geometry, both of the TE- and the TM-polarized modes are ordinary waves. Because the proton-exchange method induces a depressed ordinary index, the placement of the stress-applying region on a single side of the waveguide will not result in the leakage of the optical field in the lateral direction. Thus, the insertion loss of the polarization converter can be reduced.

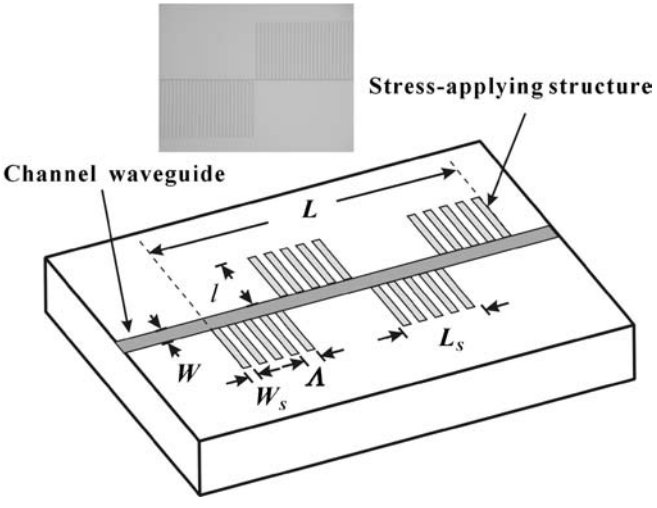

FIGURE 1 Device structure of the proposed wavelength-tunable polarization converter in x-cut $LiNbO_3$. *Inset*: a photograph of the pattern of the stress-applying structure before proton exchange

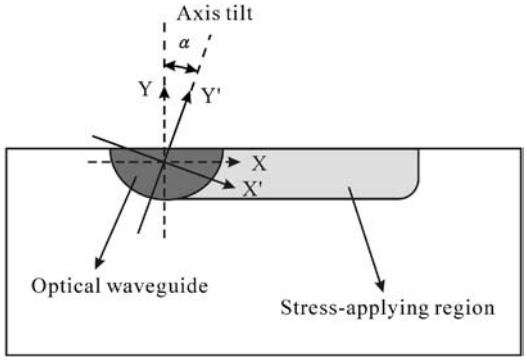

FIGURE 2 Schematic diagram of the tilt of waveguide principal axes due to the stress-applying structure produced by proton exchange

2.2 *Stress induced by proton exchange*

In the proton-exchange process, the protons diffuse into the substrate and exchange with the lithium ions in the lithium niobate as the substrate is immersed in a molten proton source, such as benzoic acid and pyrophosphoric acid. When the protons are incorporated into the lithium niobate, depending on the proton-exchange condition and the post-annealing condition, different crystallographic phases $H_xLi_{1-x}NbO_3$ are formed according to the proton concentration in the proton-exchanged layer [10]. Due to the lattice deformation, large surface stresses are induced [11] and obvious swelling phenomena on the substrate surface have been observed [12]. Because larger stress can induce a larger tilt of waveguide principal axes, the required section number or the device

length can be reduced such that more devices can be incorporated into a single substrate. Besides, since the processing temperature of proton exchange (240 °C) is far lower than that of waveguide fabrication (875 °C), the stress strength and distribution can be independently tuned by the proton-exchange process and will not affect the already-formed waveguide structure. This feature facilitates tuning the stress strength independently, and thus the tilt angle of waveguide principal axes, to completely satisfy the principle of birefringent chain filters. Therefore, the proposed polarization converter has the potential to achieve complete polarization conversion when utilizing this exclusive stress-tuning ability.

It is found that the proton-exchanged layers in x- and z-cut $LiNbO_3$ single crystals exhibit a positive strain perpendicular to the surface [12]. Besides, the induced swelling in x-cut $LiNbO_3$ is approximately twice as large as that in z-cut $LiNbO_3$ [12]. Figure 3a–e show photographs of the substrate surface in x-cut $LiNbO_3$ before proton exchange and after proton exchange, using pure benzoic acid as the proton source, at $T = 240\,^{\circ}\mathrm{C}$ for $t_{PE} = 0.5$ h, 1 h, 4 h, and 9 h. In order to release the large stress, obvious cracks approximately along the y direction appear on the substrate surface. It is found that the degree of cracking increases with the proton-exchange time. Because the existence of cracks results in a larger propagation loss, benzoic acid diluted with lithium benzoate is used as the proton source in the proton-exchange process to avoid surface cracks. The dilution ratio R is defined as

$$R = \frac{\text{moles of } C_6H_5COOLi}{(\text{moles of } C_6H_5COOLi) + (\text{moles of } C_6H_5COOH)} \times 100\% \,. \tag{3}$$

A photograph of the substrate surface after proton exchange with the dilution ratio of 0.5% at 240 °C in a sealed bottle is shown in Fig. 3f and no cracks are observed on the substrate surface. Experimental results show that, for the dilution ratios of 0.5%, 1%, and 1.5%, the substrate surfaces remain smooth without any cracks after proton exchange at 240 °C for a time as long as 36 h. Figure 4 shows the dependence of the proton-exchange depth on the proton-exchange time at the temperature $T = 240\,^{\circ}\mathrm{C}$ for $R = 0.5\%$, 1%, and 1.5%. The corresponding diffusion coefficients are $1.534 \times 10^{-2}\ \mu m^2/h$, $1 \times 10^{-2}\ \mu m^2/h$, and $8.8 \times 10^{-3}\ \mu m^2/h$. In optical measurement for the strain-optic effect, the stress-applying region with $l = 300\ \mu m$, $W_S = 5\ \mu m$, and $\Lambda = 20\ \mu m$, which is produced by proton exchange at 240 °C, is fabricated on a single side of the nickel-diffused waveguide. The waveguide is formed by diffusing a nickel strip of width $w = 4\ \mu m$ and thickness $\tau = 460$ Å into the $LiNbO_3$ substrate at the diffusion temperature $T = 875\,^{\circ}\mathrm{C}$ for the diffusion time $t = 30$ min. The related optical parameters are measured at the wavelength $\lambda = 632.8$ nm. After appending the stress-applying structure to the waveguide, waveguide principal axes are observed to be tilted toward the stress-applying structure. The dependence of the tilt angle of waveguide principal axes on the proton-exchange time for different dilution ratios is shown in Table 1. It is found that the tilt angle of waveguide principal axes increases with the proton-exchange time and decreases with the dilution ratio. In order to have a larger tilt angle of waveguide principal axes, in the following experiment, the dilution

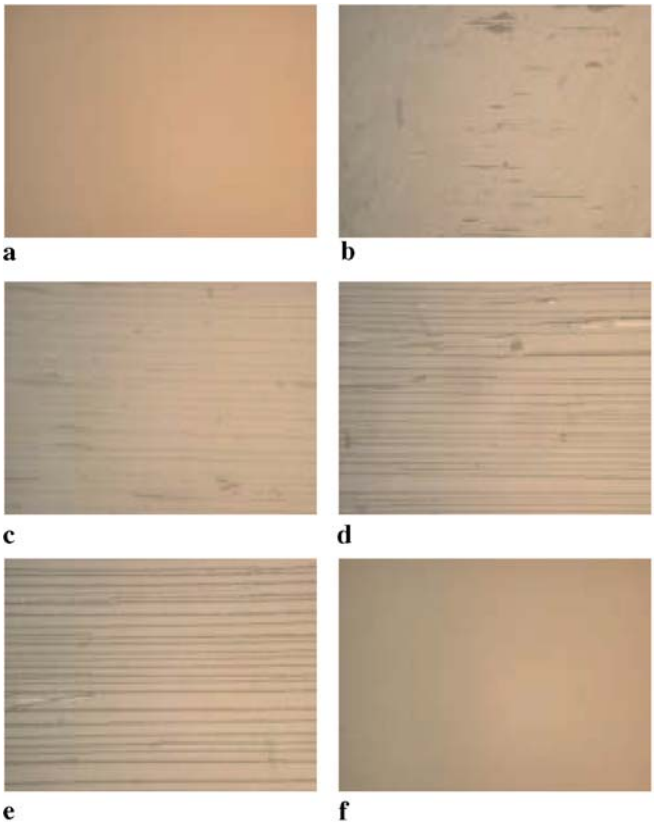

FIGURE 3 Photographs of the substrate surface. **a** before proton exchange; **b–e** after proton exchange without dilution at 240 °C for 0.5 h, 1 h, 4 h, and 9 h; **f** after proton exchange with the dilution ratio of 0.5% at 240 °C for 9 h

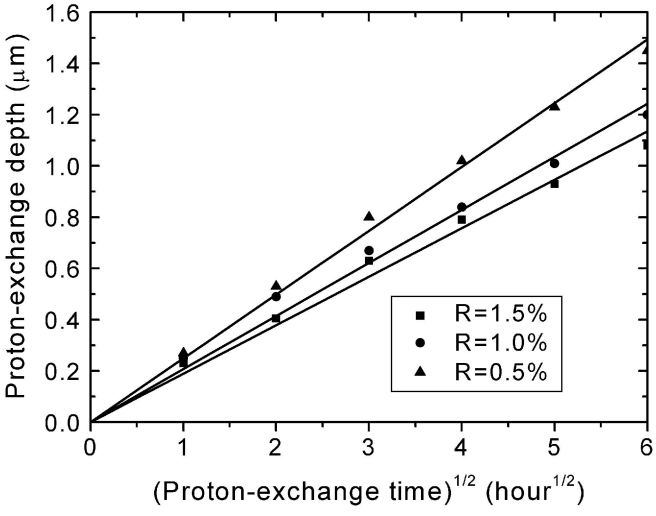

FIGURE 4 Dependence of the proton-exchange depth on the proton-exchange time for the dilution ratios $R = 0.5\%$, 1.0%, and 1.5%

Proton-exchange time	Dilution ratio $R = 0.5\%$	$R = 1\%$	$R = 1.5\%$
$t_{PE} = 1$ h	17°	15°	14°
$t_{PE} = 4$ h	20°	17°	17°
$t_{PE} = 9$ h	21°	19°	18°
$t_{PE} = 16$ h	22°	21°	19°

TABLE 1 The tilt angle of waveguide principal axes for the stress-applying structure produced by proton exchange with different dilution ratios R and proton-exchange times t_{PE}

ratio $R = 0.5\%$ is used. Besides, these α values are somewhat reduced as the waveguide length is less than 2 mm. Because of the dependence of α on the waveguide length, proposed polarization converters with section numbers $m = 2$, 3, and 4 are fabricated. Due to the better performance for the devices with $m = 4$, the results for these devices are presented in the following. A Soleil–Babinet compensator and Glan–Taylor polarizers are used in the birefringence measurement. The measured waveguide birefringence ($|n_{TE} - n_{TM}|$) has the values of 1.94×10^{-4}, 1.92×10^{-4}, and 1.89×10^{-4} for $t_{PE} = 1$ h, 4 h, and 9 h, respectively. The length of the half-wave section can be found by substituting these values into (1). For a waveguide birefringence of 1.89×10^{-4}, the overall device length with $m = 4$ is 6.696 mm. In brief, as the proton-exchange time increases, the tilt angle becomes larger and its birefringence diminishes. The propagation loss of the nickel-diffused waveguide measured by the cut-back method is 1.0 dB/cm for both of the TE and the TM polarizations. As the stress-applying structure is appended, the propagation loss increases by 0.1 dB/cm. For comparison, simultaneous diffusion of the nickel film with the pattern of the waveguide and the stress-applying structures is made. The measurement results show that α is 11° and its propagation loss is larger than that of the waveguide without the stress-applying structure by 1.59 dB/cm. The larger propagation loss is due to the index increase in the stress-applying region formed by nickel diffusion, which results in the leakage of the optical field in the lateral direction. Hence, using the proton-exchange method to produce the stress-applying structure has the advantages of large tilt angle, low propagation loss, and independent stress-tuning ability.

2.3 *Fabrication process and measurement*

The proposed polarization converters are fabricated on an x-cut, z-propagating $LiNbO_3$ substrate. First, nickel-diffused waveguides are produced by diffusing nickel strips of width $w = 4$ μm and thickness $\tau = 460$ Å into the substrate at 875 °C for 30 min. As the proton-exchange mask, an aluminum film of thickness 3000 Å is deposited and patterned with a shape of the stress-applying region. Then, the substrate is put in the diluted benzoic acid with the dilution ratio $R = 0.5\%$ for proton exchange to produce the stress-applying structure. After proton exchange, the substrate is cleaned and the aluminum film is removed by the diluted hydrochloric acid. Before measurement, both ends of the substrate are polished for end-fire coupling. In the device measurement, a tunable external-cavity semiconductor laser with a wavelength-tuning range from 631 nm to 639 nm is used as a light source. A temperature controller with a resolution of 0.1 °C controls the device temperature. The polarization-conversion efficiency is defined as the ratio of the optical power in the converted polarization to the total optical power at the converter output.

3 Results and discussion

The dependence of the polarization-conversion efficiency on the proton-exchange time for the dilution ratios $R = 0.5\%$, 1.0%, and 1.5% is shown in Fig. 5. It is found that the polarization-conversion efficiency initially increases with the proton-exchange time and gradually approaches a constant value. As the proton-exchange time increases, the stress-applying region becomes deeper and more optical field can be incorporated into the stress-distributed region, i.e. the region with the tilt of waveguide principal axes. Consequently, the overlap integral between the optical field distribution and the stress distribution increases and the polarization conversion becomes more efficient. When most of the optical field is included in the stress-distributed region, the polarization-conversion efficiency no longer increases rapidly and gradually approaches a saturated value. The proton exchange with a larger dilution ratio results in a slower proton-exchange rate and a smaller tilt angle of waveguide principal axes. Because of a slower proton-exchange rate for a larger dilution rate, the rate of increase of the polarization-conversion efficiency is smaller. When the proton-exchange time increases to a certain extent such that most of the optical field is contained in the stress-distributed region, a smaller polarization-conversion efficiency for a larger dilution ratio is due to its smaller tilt angle of waveguide principal axes, which causes an insufficient polarization conversion. The polarization-conversion efficiencies for the polarization conversion from the TM- to the TE-polarized mode and from the TE- to the TM-polarized mode are almost equal with a difference of less than 3%, as indicated from a comparison with the results in Fig. 5.

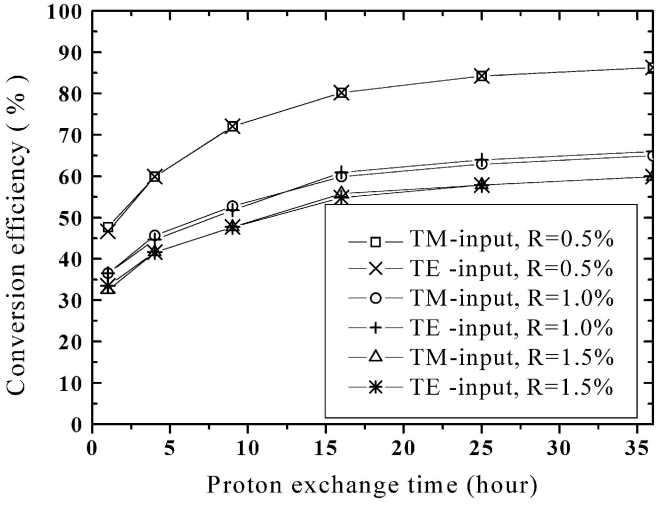

FIGURE 5 Dependence of the polarization-conversion efficiency for the TM- and the TE-polarization inputs on the proton-exchange time. The stress-applying structure is formed by proton exchange at 240 °C with the dilution ratios $R = 0.5\%$, 1.0%, and 1.5%

The device parameters of the proposed polarization converter are designed according to the measurement results of the waveguide birefringence and the tilt angle of waveguide principal axes at the wavelength $\lambda = 632.8$ nm. Experimental results show that the waveguide birefringence and the tilt angle of waveguide principal axes are slightly dependent on the length of the stress-applying region. As the length is smaller than 1 mm, it is difficult to produce the required samples and measure the related parameters required in the device design. Hence, the related measurement can only be done for waveguides of length larger than 1 mm. These errors result in a deviation of the calculated value of L_S and the section number, which cause the phase-match condition and the principle

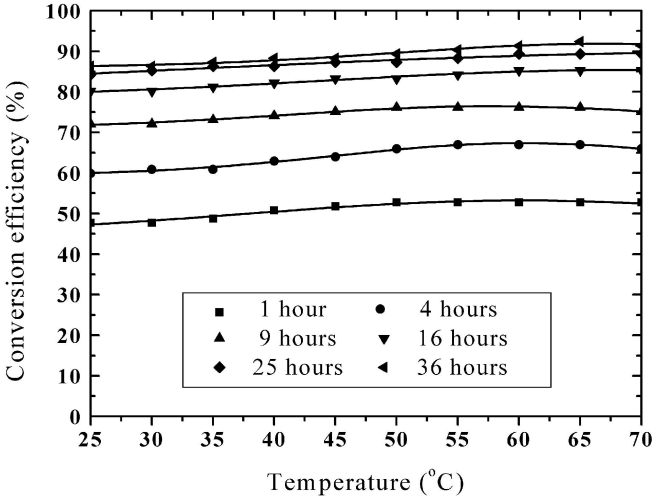

FIGURE 6 Dependence of the polarization-conversion efficiency on the device temperature. The stress-applying structure is formed by proton exchange at 240 °C for 1–36 h

of the birefringent chain filters not to be completely satisfied. These deviations can be partially compensated by the thermal-optic effect. Figure 6 shows the effect of temperature on the polarization-conversion efficiency. For devices produced by different proton-exchange times, the polarization-conversion efficiency obviously increases by about 5%. This improvement is attributed to the more complete phase-matched coupling through the thermal index tuning and the thermal expansion of the material. The complete polarization conversion is not achieved as a result of the deviation from the optimal tilt angle of waveguide principal axes.

Figure 7 shows the wavelength dependence of the polarization-conversion efficiency at the temperatures $T = 25\,^{\circ}\mathrm{C}$ and 70 °C for the polarization converter produced with the proton-exchange times $t_{\mathrm{PE}} = 25$ h and 36 h. For $t_{\mathrm{PE}} = 25$ h, the wavelength of maximum conversion at $T = 25\,^{\circ}\mathrm{C}$ is around 637 nm. When the temperature rises to 70 °C, the corresponding wavelength is shifted to 633 nm. As to $t_{\mathrm{PE}} = 36$ h, the wavelength of maximum conversion is shifted from 636.2 nm at $T = 25\,^{\circ}\mathrm{C}$ to 633 nm at $T = 70\,^{\circ}\mathrm{C}$. The maximum polarization-conversion efficiencies are 90.38% and 92.41% for $t_{\mathrm{PE}} = 25$ h and 36 h, respectively. The better polarization-conversion efficiency for $t_{\mathrm{PE}} = 36$ h is due to the larger overlap integral between the optical field distribution and the stress distribution. The thermal-optic tuning characteristics for the proposed polarization converter are shown in Fig. 8. The wavelength tuning by the thermal-optic effect is almost linear and has tuning rates of -0.112 nm/°C and -0.115 nm/°C for $t_{\mathrm{PE}} = 25$ h and 36 h, respectively. The corresponding polarization-conversion efficiency for the wavelength range from 632 nm to 638 nm is between 88.35% and 92.41%. The polarization conversion is not complete (100%) as a result of a slight deviation from the principle of the birefringence chain filters. The insertion loss of the proposed polarization converter is 0.73 dB.

The polarization-conversion efficiency is dependent on: (1) the overlap integral between the optical field distribution and the stress distribution and (2) the satisfaction levels of the phase-match condition and the principle of the birefringent chain filters. For the proposed polarization converter, the interaction between the optical field and the strain can be improved by increasing the proton-exchange depth, which can be achieved simply by prolonging the proton-exchange time or raising the proton-exchange temperature. The field mode size in the waveguide is larger for the longer wavelength, e.g. 1310 nm or 1550 nm used in optical communication. In order to have a large overlap integral between the optical field distribution and the stress distribution, the required stress distribution for the devices operated at the longer wavelength needs to be deeper than that at the shorter wavelength. For the proposed device, the depth of the stress distribution can be easily enlarged by increasing the proton-exchange depth. After re-designing the device parameters, the proposed polarization converter still has high polarization-conversion efficiency when applied at the communication wavelength. Besides, the stress distribution and its strength in the stress-applying structure can be independently fine tuned without affecting the waveguide characteristics by annealing after proton exchange or varying the dilution ratio of benzoic acid, such that the principle of the birefringent chain filters can be completely satisfied. Hence, the proposed polarization converter has a high parameter-tuning feasibil-

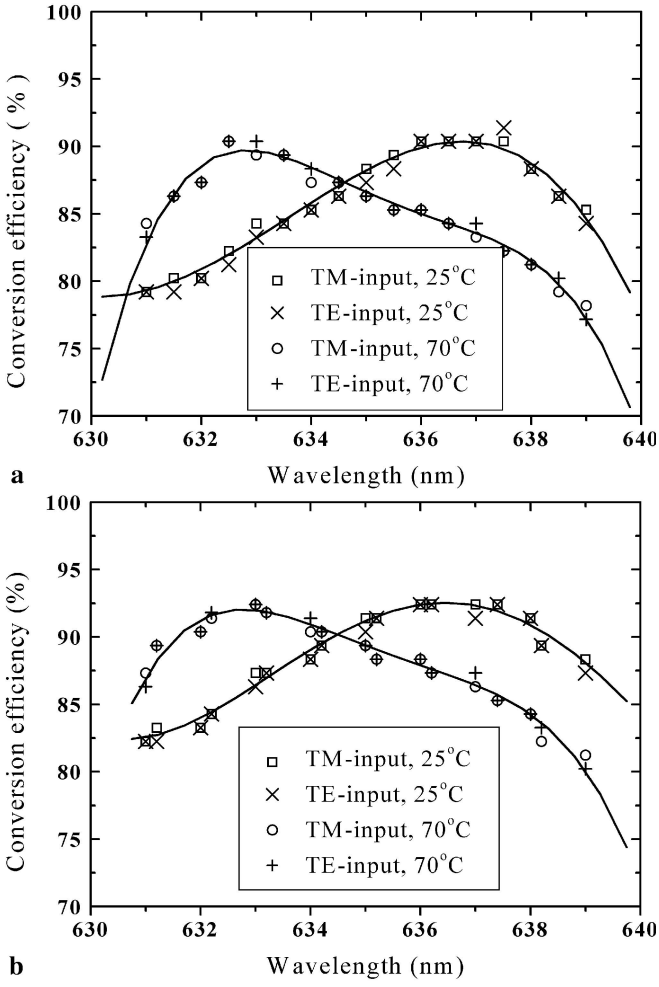

FIGURE 7 The polarization-conversion efficiency versus the wavelength for the temperatures $T = 25\,^{\circ}\mathrm{C}$ and 70 °C for the proposed polarization converter produced with the proton-exchange times: **a** $t_{\mathrm{PE}} = 25$ h; **b** $t_{\mathrm{PE}} = 36$ h

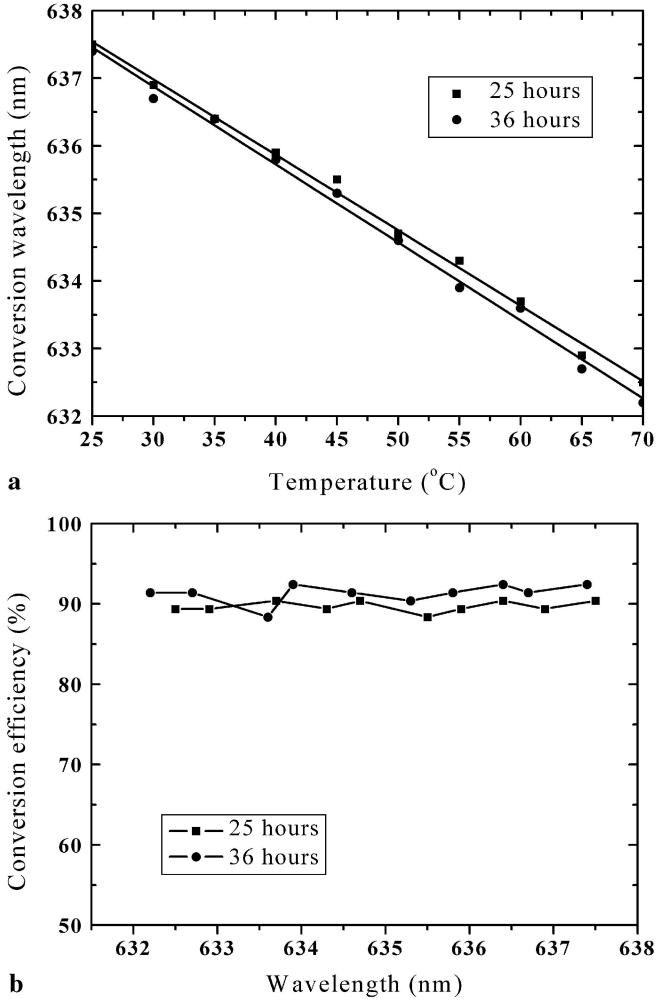

FIGURE 8 Thermal-optic tuning characteristics of the proposed polarization converter produced with the proton-exchange times $t_{PE} = 25$ h and 36 h. **a** The wavelength of maximum conversion versus the device temperature. **b** The polarization-conversion efficiency versus the wavelength of maximum conversion

ity and its polarization-conversion efficiency can be further enhanced.

4 Conclusions

A new wavelength-tunable polarization converter in x-cut $LiNbO_3$ using the strain-optic effect has been successfully demonstrated. Different fabrication techniques in lithium niobate are used to satisfy the requirement of exclusive characteristics in different device regions. The problem of surface cracking due to proton exchange in x-cut $LiNbO_3$ can be overcome by diluting the proton source. Experimental results show that, for the dilution ratios of 0.5%, 1%, and 1.5%, the substrate surfaces remain smooth without any cracks after proton exchange at 240 °C for a time as long as 36 h. The stress induced by the proton-exchanged region causes the tilt of waveguide principal axes and thus the coupling between two orthogonal polarization modes. The device structure of the proposed polarization converter is designed according to the following considerations: (1) avoiding the stress-applying structure affecting the lateral optical confinement of the waveguide; (2) maximizing the overlap integral between the optical field distribution and the stress distribution; (3) satisfying the phase-match condition and the principle of the birefringent chain filters. The wavelength of maximum conversion can be tuned by the thermal-optic effect at tuning rates of -0.112 nm/°C and -0.115 nm/°C for the proton-exchange times of 25 h and 36 h, respectively. The maximum polarization-conversion efficiency is 92.41%, which can be further improved by optimization of the fabrication parameters.

ACKNOWLEDGEMENTS This work was supported by the National Science Council, Taipei, Taiwan, Republic of China under Contract No. NSC 93-2215-E-027-010.

REFERENCES

1 H. Porte, J.P. Goedgebuer, R. Ferriere, N. Fort: IEEE J. Quantum Electron. **QE-25**, 1760 (1989)
2 L.N. Binh, J. Livingstone, D.H. Steven: Opt. Lett. **5**, 83 (1980)
3 P.K. Tien, R.J. Martin, R. Wolfe, R.C. Le Craw, S.L. Blank: Appl. Phys. Lett. **21**, 394 (1972)
4 Z. Tang, O. Eknoyan, H.F. Taylor, V.P. Swenson: Appl. Phys. Lett. **62**, 1059 (1993)
5 T. Lang, F. Bahnmüller, P. Benech: IEEE Photon. Technol. Lett. **10**, 1295 (1998)
6 H.S. Jung, O. Eknoyan, H.F. Taylor: Jpn. J. Appl. Phys. **38**, L1406 (1999)
7 K. Merterns, B. Scholl, H.J. Scymitt: IEEE Photon. Technol. Lett. **10**, 1133 (1998)
8 J.Z. Huang, R. Scarmozzino, G. Nagy, M.J. Steel, R.M. Osgood, Jr.: IEEE Photon. Technol. Lett. **12**, 317 (2000)
9 I. Šolv: J. Opt. Soc. Am. **55**, 621 (1965)
10 C.E. Rice: J. Solid State Chem. **64**, 188 (1986)
11 M. Minakata, K. Kumagai, S. Kawakami: Appl. Phys. Lett. **49**, 992 (1986)
12 F. Zhou, A.M. Matteo, R.M. De La Rue, C.N. Ironside: Electron. Lett. **28**, 87 (1992)